Biomedical Optics EXPRESS

In vivo photothermal treatment by the peritumoral injection of macrophages loaded with gold nanoshells

Taeseok Daniel Yang,[1] Wonshik Choi,[1] Tai Hyun Yoon,[1] Kyoung Jin Lee,[1] Jae-Seung Lee,[2] Jang Ho Joo,[2] Min-Goo Lee,[3] Hong Soon Yim,[3] Kyung Min Choi,[3] Byoungjae Kim,[3] Jung Joo Lee,[4] Heejin Kim,[4] Doh Young Lee,[5] Kwang-Yoon Jung,[5] and Seung-Kuk Baek[5,*]

[1]*Korea University, Department of Physics, Seoul, South Korea*
[2]*Korea University, Department of Materials Science and Engineering, Seoul, South Korea*
[3]*Korea University, Department of Physiology, Seoul, South Korea*
[4]*LivsMedInc., Seoul, South Korea*
[5]*Korea University, Department of Otolaryngology-Head and Neck Surgery, Seoul, South Korea*
[*]*mdskbaek@gmail.com*

Abstract: Photothermal treatment methods have been widely studied for their target specificity and potential for supplementing the limitations of conventional surgical treatments. In this study, we conducted *in vivo* photothermal treatments using macrophages containing nanoshells as live vectors. We injected macrophages at the peritumoral sites and observed that they had penetrated into the tumor approximately 48 hours after injection. Afterwards, we irradiated with a near-infrared laser for 2 minutes at 1 W/cm^2, causing cancer cell death. Our study identified the optimal conditions of the photothermal treatment and confirmed the feasibility of its use in *in vivo* treatments.

OCIS codes: (170.5180) Photodynamic therapy; (350.5340) Photothermal effects; (170.0170) Medical optics and biotechnology.

References and links

1. L. R. Hirsch, R. J. Stafford, J. A. Bankson, S. R. Sershen, B. Rivera, R. E. Price, J. D. Hazle, N. J. Halas, and J. L. West, "Nanoshell-mediated near-infrared thermal therapy of tumors under magnetic resonance guidance," Proc. Natl. Acad. Sci. U.S.A. **100**(23), 13549–13554 (2003).
2. I. H. El-Sayed, X. Huang, and M. A. El-Sayed, "Selective laser photo-thermal therapy of epithelial carcinoma using anti-EGFR antibody conjugated gold nanoparticles," Cancer Lett. **239**(1), 129–135 (2006).
3. S. K. Baek, A. R. Makkouk, T. Krasieva, C. H. Sun, S. J. Madsen, and H. Hirschberg, "Photothermal treatment of glioma; an *in vitro* study of macrophage-mediated delivery of gold nanoshells," J. Neurooncol. **104**(2), 439–448 (2011).
4. J. A. Schwartz, A. M. Shetty, R. E. Price, R. J. Stafford, J. C. Wang, R. K. Uthamanthil, K. Pham, R. J. McNichols, C. L. Coleman, and J. D. Payne, "Feasibility study of particle-assisted laser ablation of brain tumors in orthotopic canine model," Cancer Res. **69**(4), 1659–1667 (2009).
5. G. S. Terentyuk, G. N. Maslyakova, L. V. Suleymanova, N. G. Khlebtsov, B. N. Khlebtsov, G. G. Akchurin, I. L. Maksimova, and V. V. Tuchin, "Laser-induced tissue hyperthermia mediated by gold nanoparticles: toward cancer phototherapy," J. Biomed. Opt. **14**(2), 021016 (2009).
6. H. Maeda, J. Fang, T. Inutsuka, and Y. Kitamoto, "Vascular permeability enhancement in solid tumor: various factors, mechanisms involved and its implications," Int. Immunopharmacol. **3**(3), 319–328 (2003).
7. H. F. Dvorak, "Leaky tumor vessels: consequences for tumor stroma generation and for solid tumor therapy," Prog. Clin. Biol. Res. **354A**, 317–330 (1990).
8. H. Otsuka, Y. Nagasaki, and K. Kataoka, "PEGylated nanoparticles for biological and pharmaceutical applications," Adv. Drug Deliv. Rev. **55**(3), 403–419 (2003).
9. S. J. Madsen, S. K. Baek, A. R. Makkouk, T. Krasieva, and H. Hirschberg, "Macrophages as cell-based delivery systems for nanoshells in photothermal therapy," Ann. Biomed. Eng. **40**(2), 507–515 (2012).
10. E. S. Glazer, C. Zhu, K. L. Massey, C. S. Thompson, W. D. Kaluarachchi, A. N. Hamir, and S. A. Curley, "Noninvasive radiofrequency field destruction of pancreatic adenocarcinoma xenografts treated with targeted gold nanoparticles," Clin. Cancer Res. **16**(23), 5712–5721 (2010).
11. W. D. James, L. R. Hirsch, J. L. West, P. D. O'Neal, and J. D. Payne, "Applications of INAA to the build-up and clearance of gold nanoshells in clinical studies in mice," J. Radioanal. Nucl. Chem. **271**(2), 455–459 (2007).

#254667 Received 27 Nov 2015; accepted 11 Dec 2015; published 18 Dec 2015

12. M. R. Choi, K. J. Stanton-Maxey, J. K. Stanley, C. S. Levin, R. Bardhan, D. Akin, S. Badve, J. Sturgis, J. P. Robinson, R. Bashir, N. J. Halas, and S. E. Clare, "A cellular Trojan Horse for delivery of therapeutic nanoparticles into tumors," Nano Lett. **7**(12), 3759–3765 (2007).
13. J. C. Kah, K. Y. Wong, K. G. Neoh, J. H. Song, J. W. Fu, S. Mhaisalkar, M. Olivo, and C. J. Sheppard, "Critical parameters in the pegylation of gold nanoshells for biomedical applications: an *in vitro* macrophage study," J. Drug Target. **17**(3), 181–193 (2009).
14. R. D. Leek, C. E. Lewis, R. Whitehouse, M. Greenall, J. Clarke, and A. L. Harris, "Association of macrophage infiltration with angiogenesis and prognosis in invasive breast carcinoma," Cancer Res. **56**(20), 4625–4629 (1996).
15. R. D. Leek, R. J. Landers, A. L. Harris, and C. E. Lewis, "Necrosis correlates with high vascular density and focal macrophage infiltration in invasive carcinoma of the breast," Br. J. Cancer **79**(5-6), 991–995 (1999).
16. S. J. Madsen, C. Christie, S. J. Hong, A. Trinidad, Q. Peng, F. A. Uzal and H. Hirschberg, "Nanoparticle-loaded macrophage-mediated photothermal therapy: potential for glioma treatment," Lasers Med. Sci. **30**, 1357–1365 (2015).
17. T. D. Yang, W. Choi, T. H. Yoon, K. J. Lee, J. S. Lee, S. H. Han, M. G. Lee, H. S. Yim, K. M. Choi, M. W. Park, K. Y. Jung, and S. K. Baek, "Real-time phase-contrast imaging of photothermal treatment of head and neck squamous cell carcinoma: an *in vitro* study of macrophages as a vector for the delivery of gold nanoshells," J. Biomed. Opt. **17**(12), 128003 (2012).
18. S. Valable, E. L. Barbier, M. Bernaudin, S. Roussel, C. Segebarth, E. Petit, and C. Rémy, "*In vivo* MRI tracking of exogenous monocytes/macrophages targeting brain tumors in a rat model of glioma," Neuroimage **40**(2), 973–983 (2008).
19. R. D. Oude Engberink, E. L. Blezer, E. I. Hoff, S. M. van der Pol, A. van der Toorn, R. M. Dijkhuizen, and H. E. de Vries, "MRI of monocyte infiltration in an animal model of neuroinflammation using SPIO-labeled monocytes or free USPIO," J. Cereb. Blood Flow Metab. **28**(4), 841–851 (2008).
20. S. C. Gad, K. L. Sharp, C. Montgomery, J. D. Payne, and G. P. Goodrich, "Evaluation of the toxicity of intravenous delivery of auroshell particles (gold-silica nanoshells)," Int. J. Toxicol. **31**(6), 584–594 (2012).

1. Introduction

Photothermal treatment (PTT) aims to destroy cancers by converting photon energy into heat via nanoparticles [1–5]. In recent years, interest in PTT has increased due to the development of novel nanoparticles with improved target specificities and heat conversion efficiencies. In addition, the functionalities of the nanoparticles have improved. For example, nanoparticles are now often coated with chains of polyethylene glycol (PEG) to enhance their permeability and retention (EPR) effect for immature tumor vasculature [6,7]. This has resulted in increased circulation times [8,9] and increased accumulation of nanoparticles in the tumor. Tumor-specific antibodies such as those targeting the epidermal growth factor receptor (EGFR) were often conjugated on the nanoparticle surface to enhance target specificity [10]. Even with these efforts, however, high concentrations of nanoparticles were observed in the liver and spleen, and only a small fraction of the injected dose of nanoparticles reached the tumor [11]. Those nanoparticles that diffused into healthy tissue may also produce heat by laser irradiation, and damage that healthy tissue. Therefore, it is necessary to improve the target specificity of nanoparticle delivery.

One alternative method that has drawn attention is the use of macrophages as live vectors [9,12,13]. The macrophages can phagocytize nanoparticles and then carry them to target sites. Although they have no direct specificity for cancer cells, they are phagocyte scavenger cells and have the ability to trace the signals released by cells undergoing necrosis. Accordingly, they may preferentially penetrate into hypoxic regions within the tumor mass [14,15]. Most previous studies were confined to *in vitro* studies [16]. In our last study, we confirmed the possibility of using macrophages as live vectors for the delivery of nanoparticles and identified the optimal conditions for PTT to selectively kill cancer cells around nanoshell (NS)-loaded macrophages in an *in vitro* model [17]. It is only recently that the feasibility of the *in vivo* treatments has been investigated. For example, Hirschberg *et al*. showed that brain tumors can be removed with relatively long irradiation by near-infrared (NIR) light. In their study, glioma cells were injected near the surface of rat brains, and NS-loaded macrophages were injected directly to the tumor sites. Laser irradiation was administrated right after macrophage injection. This intratumoral injection is a straightforward way of delivering NSs to tumor sites. However, since the macrophages may have difficulty spreading throughout tumor masses, the thermal effects can be localized to the site of injection.

#254667 Received 27 Nov 2015; accepted 11 Dec 2015; published 18 Dec 2015

In our present study, we performed *in vivo* animal studies for head and neck cancer. We prepared tumor sites by planting SNU-1041 squamous cancer cells into the necks of mice and waited about 2 weeks until the diameter of the tumor reached approximately 0.5 cm. We injected the macrophages into peritumoral sites rather than directly into the tumors to spread the macrophages throughout the tumor mass. We took this approach because we had found in a separate study that it takes macrophages approximately 48 hours to penetrate into the tumor, and observed that they distribute more evenly after peritumoral than intratumoral injection. After 48 hours of injection, irradiation was done by NIR laser and the effectiveness of the PTT treatment was verified by immunohistochemistry. The optimal condition of 960 nm NIR irradiation for inducing cancer cells death was 1 W/cm^2 over 2 minutes. We also confirmed that the nanoparticles aggregated after the treatment and stayed on site, which suggests that the toxicity associated with nanoparticle circulation can be alleviated by our injection methods. The experimental parameters of the injection methods, and the timing, power and duration of the irradiation identified by our study serve as a baseline when further enhancing the feasibility of photothermal treatment.

2. Materials and methods

We conducted the *in vivo* PTT experiment following the illustration shown in Fig. 1. We separately prepared macrophages and nanoshells, and then incubated them together so that the macrophages could phagocytose the NSs. We then injected NS-loaded macrophages into either peritumoral or intratumoral sites. After waiting about 48 hours for the cells to migrate into the tumors, we performed PTT by irradiating the tumor sites with 960 nm NIR laser (IPG Photonics, Oxford, Massachusetts). To assess the effect of the treatment, an immunohistochemical analysis was conducted either directly after or 2 weeks after the PTT. Next, we explain in detail the preparation of the materials and experimental methods.

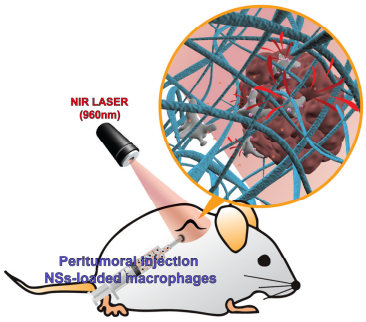

Fig. 1. An illustration of the *in vivo* PTT study. NS-loaded macrophages were injected into peritumoral sites. After waiting for about 48 hours, a 960 nm NIR laser irradiated to the tumor sites for 2 minutes with a 1 W/cm^2 intensity and a laser spot size 1.2 cm in diameter.

2.1 Preparation of nanoshells (NSs)

Gold chloride trihydrate ($HAuCl_4$•$3H_2O$, cat.# 520918), ammonium hydroxide solution (30% NH_3 as NH_4OH assay, cat.# 221228), ethanol (cat.# 459828), tetraethyl orthosilicate (TEOS, cat.# 333859), sodium hydroxide (NaOH, cat.# 306576), tetrakis (hydroxymethyl) phosphonium chloride solution (THPC, 80% aqueous solution, cat.# 404861), (3-aminopropyl)trimethoxysilane (APTMS, cat.# 281778), potassium carbonate (cat.# 367877), and formaldehyde solution (cat.# F8775) were purchased from Sigma-Aldrich (USA). Ultrapure water from a Millipore Direct-Q3 system (18.2 MΩ•cm, Massachusetts, USA) was used. The UV-Vis-NIR spectra of the nanoparticles were obtained using a Cary 5000 ultraviolet-visible-NIR (UV-Vis-NIR) spectrophotometer.

The core silica particles were synthesized following a modified Stöber method. In brief, an ammonium hydroxide solution (3.5 mL, 30% NH_3 as NH_4OH assay) was added to 50 mL of

#254667 Received 27 Nov 2015; accepted 11 Dec 2015; published 18 Dec 2015

ethanol. The mixture was vigorously stirred, as 1.5 mL TEOS was added in a dropwise manner. As the reaction proceeded, the mixture solution became increasingly opaque, which indicated silica particle formation. The mixture was stirred continuously for 30 min. The impurities, primarily unreacted reagents, were removed by discarding the supernatant after centrifugation at 4600 g for 15 min. Finally, the silica particles were dispersed in water.

To form the shell, primarily of 2-3 nm gold nanoparticles, around the much larger silica nanoparticles, the silica surface was first amine-functionalized and reacted with gold particles which would play the role of nucleation sites for shell growth. To activate the surface of the silica nanoparticles using amine groups, 16.87 μL of APTMS was added to 50 mL of the silica nanoparticle solution under vigorous stirring, which was continued for 1 h. Amine-functionalized silica nanoparticles were washed from the unreacted chemicals by centrifugation at 4600 g for 15 min, removal of the supernatant, and re-dispersion in pure water. The tiny gold nanoparticles were separately synthesized by rapidly combining, while stirring, an aqueous $HAuCl_4$ solution (2 mL, 27 mM) with a mixture containing pure water (45 mL), aqueous NaOH solution (0.5 mL, 1 M), and THPC prepared by adding 12 μL of an 80% THPC aqueous solution to 1 mL water. After 5 min this procedure had produced a dark brown gold nanoparticle solution.

500 μL of the amine-functionalized silica nanoparticle solution was added to 5 mL of the gold nanoparticle solution. The mixture was shaken gently for 5 min, allowed to sit for 2 h, centrifuged at 4600 G for 15 min, and redispersed in pure water. At this point, the particles appeared brown-red because of the color of the attached gold nanoparticles.

To prepare the growth solution for the gold NS, 0.025 g of potassium carbonate was dissolved in 100 mL water and stirred for 10 min, and then 1.5 mL of 27 mM $HAuCl_4$ solution was added. Once the yellow growth solution had become clear, a mixture containing 4 mL of the growth solution and 200 μL of the gold nanoparticle-amine-silica nanoparticle solution was combined with 27 μL of formaldehyde. The mixture turned blue, which indicated the formation of the NSs. Once formed, the NSs were finally suspended in pure water. The silica core–gold shell nanoparticles were analyzed by transmission electron microscopy (TEM). They have a silica core (157 nm in diameter) that was evenly coated with a thin gold NS (14 nm thick) [17].

2.2 Preparation of cancer cells and mouse peritoneal macrophages

The SNU-1041 squamous cancer cell line which is derived from human pharyngeal cancer was cultured in a mixture of 500 mL RPMI 1640 (Gibco BRL, Grand Island, New York) and 50 mL fetal bovine serum (Gibco BRL) in a 5% CO_2 incubator. In addition, the peritoneal macrophages were prepared from 6 to 8 week old outbred mice from the Institute for Cancer Research (ICR) which had been intraperitoneally injected with 10 mL of phosphate-buffered saline solution (PBS). The macrophages were isolated from the PBS cell suspension by adding a red blood cell (RBC) lysis buffer followed by centrifugation. After the peritoneal macrophages were allowed to adhere to the culture dish for 2 h, the cultures were washed twice with RPMI 1640 to remove non-adherent cells and the adhered macrophages were collected using cell scrapers (SPL Life Sciences, Korea). These studies were performed according to an Animal Medical Center Institutional Review Board approved protocol.

2.3 Uptake of NSs by the peritoneal macrophages

In the previous *in vitro* study [17], we found that for optimal PTT performance the concentration of NSs should be around 27.5 pM and the number of macrophage cells should be 2×10^4 cells. The NS suspension was co-incubated with peritoneal macrophages with gentle shaking in a 15-mL tube for 1 hour. The mixture containing the NSs and macrophages was seeded onto a 35-mm cell culture dish and incubated for 2 hours to allow the cells to settle and adhere to the bottom. We then rinsed the cultures three times with a Hanks' balanced salt solution containing calcium chloride and magnesium chloride (HBSS, Gibco, Carlsbad, California) to remove the NSs that had not been ingested by the macrophages. The

#254667 Received 27 Nov 2015; accepted 11 Dec 2015; published 18 Dec 2015

NS-loaded macrophages adhered to the bottom were collected with cell scrapers. Finally, we obtained a cell suspension with 1×10^4 cells/mL of the NS-loaded macrophages.

2.4 Xenotransplantation of the cancer cell line

All animal experiments were performed according to an Institutional Animal Care and Use Committee approved protocol. The concentration of the SNU-1041 squamous cancer cell line was diluted to 10^8 cells/mL, and the cells were injected into the backs of the nude mice (BALB/c-nu/nu, male, aged 5 weeks) using a 1-mL insulin syringe. Animal body weights and physical symptoms were monitored during the experiments. The tumor size was measured three times per week, and PTT was performed when the maximal diameter of the tumor became greater than 5 mm.

2.5 Photothermal treatment (PTT) on the xenograft nude mouse

The NS-loaded macrophages were applied in a xenograft nude mouse using two types of local injection – intratumoral and peritumoral. For the intratumoral injection, 10 μL of NS-loaded macrophage (1×10^4 cells/mL) was injected into the mid-portion of the xenograft tumor mass. 48 hours after the injection, a 960 nm NIR laser with an irradiance of 1 W/cm^2, and a laser spot diameter of 1.2 cm illuminated the tumor sites for 2 minutes. In the case of the peritumoral injection, 10 μL of NS-loaded macrophages (1×10^4 cells/mL) was injected at four locations surrounding the xenograft tumor mass, and 48 hours after the injection, the same irradiation dose as for the intratumoral experiment was administered to the tumor sites. The irradiated xenograft tumor masses were resected and subsequently examined via conventional hematoxylin and eosin (H&E) staining.

3. Results and discussion

3.1 Identification of the migration of macrophages into tumor xenograft

Before administering the PTT, we investigated the migration of the macrophages into the tumor xenograft. At first, we traced the movements of bare macrophages with no NSs. The macrophages were labeled with the cell-labeling solution (Vybrant Dio, Molecular Probes, Inc.), which has a distinctively visible fluorescence property, low cytotoxicity, and a high resistance to intercellular transfer. The macrophages were injected into either intratumoral or peritumoral sites. 12, 24, or 48 hours after the injection, we dissected a xenograft tumor mass with the adjacent soft tissue, including skin, subcutaneous tissue, and muscles. The removed tissues were fixed with 4% paraformaldehyde solution and cryopreserved in a 30% sucrose solution. The tissues embedded with optimal cutting temperature compound were cut into 4-μm thick tissue sections using a cryostat and examined with a fluorescence microscope to identify the movement of labeled macrophages. The macrophages injected at the center of the xenograft tumor (the intratumoral injection group) showed minimal migration from the injection site even 48 hours after the injection (Fig. 2(A)). In contrast, the macrophages in the peritumoral injection group were alive and had invaded through the capsule into the tumor interior after injection. We observed that they had spread further after 48 hours than after 12 or 24 hours (Fig. 2(B), 2(C) and 2(D)).

#254667 Received 27 Nov 2015; accepted 11 Dec 2015; published 18 Dec 2015

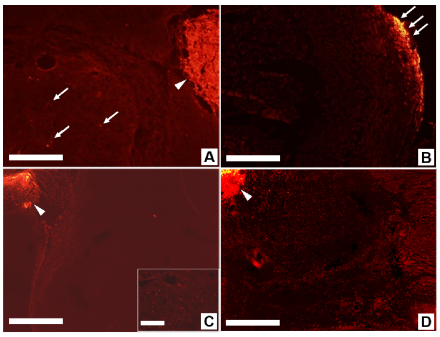

Fig. 2. Migration of fluorescence-labeled macrophages in xenograft tumors. (A) Intratumoral injection of macrophage. Xenograft tumor with labeled macrophages injected inside shows the migration of a few macrophages (arrow) from the injection site (arrowhead). Scale bar is 100 μm.(B) 12 hours after peritumoral injection of macrophage, the Xenograft tumor capsule image shows accumulation of labelled macrophages (arrows). Scale bar is 200 μm. (C) 24 hours after peritumoral injection the tumor image shows that some macrophages have migrated from the injection site (arrowhead) into the tumor, as visible in the inset. Scale bars are 500 μm and 100 μm. (D) 48 hours after peritumoral injection, the macrophages have extensively migrated (bright red dots) from the injection site (arrowhead) into the tumor. Scale bar is 500 μm.

We then performed immunohistochemical studies to identify the migration of the NS-loaded macrophages. They could not be identified with a fluorescence staining method because fluorescence was quenched by the surface plasmon polaritons induced around the nanoshells. Instead, we stained the macrophages and tissues with H&E staining after performing PTT for a duration ensuring the tumor cells were not completely destructed. Ten μL of NS-loaded macrophages (1×10^4 cells/mL) were injected at four locations surrounding the xenograft tumor mass. 48 hours after the injection of the NS-loaded macrophages, the general area of the tumor mass was irradiated for 30 seconds with a 960-nm NIR laser at an irradiance of 1 W/cm^2 and a laser spot size of 1.2 cm in diameter. 24 hours after PTT, the xenograft mice were put down, and the tumor tissues extracted. The resected xenograft tumor mass was fixed with 4% paraformaldehyde in 0.1 mol/L PBS (pH 7.4) overnight at 4°C and embedded in paraffin for immunohistochemical staining. Prior to staining, the 4-μm-thick sections were deparaffined and rehydrated in xylene and graduated dilutions of ethanol. Immunohistochemical analysis was performed by the avidin-biotin-peroxidase (ABC) method (Vectastain ABC-Elite kit, Vector Laboratories, Burlingame, California). A rat monoclonal anti-F4/80 antibody (1:100 dilution, Santa Cruz Biotechnology, Texas, USA) was used to identify macrophages and the distribution of peroxidase was revealed by incubating the sections in a solution containing 3,3′-diaminobenzidine tetrahydrochloride (Sigma, St Louis, Missouri). The slides were counterstained with hematoxylin and subsequently mounted.

In the xenograft tumors injected with NS-loaded macrophages and exposed to PTT, the majority of the injected macrophages stayed near the injection site (Fig. 3(B)). However, quite a number of them were found inside the tumor (Fig. 3(C)), indicating that some of the injected NS-loaded macrophages had moved from the peritumoral injection site to the inside of the tumor.

As a point of reference, we surveyed an immunohistochemical image of a xenograft tumor from a nude mouse which had not been injected with NS-loaded macrophages, and found in situ macrophages inside the tumor as well as near the border between the tumor and its adjacent tissues (Fig. 3(A)). This suggests that macrophages are attracted to the tumor sites intrinsically.

We could also observe the fate of NSs after PTT. As shown in Fig. 3(D), after PTT the NSs aggregated into coarse particles of approximately 10μm. Presumably, the NSs aggregated into coarse particles cannot be passively distributed to other organs. This result means that the local injection of NSs might overcome the cytotoxicity problem which is caused by the uncontrollable circulation of nanoparticles, such as after intravenous injection [18–20].

#254667 Received 27 Nov 2015; accepted 11 Dec 2015; published 18 Dec 2015

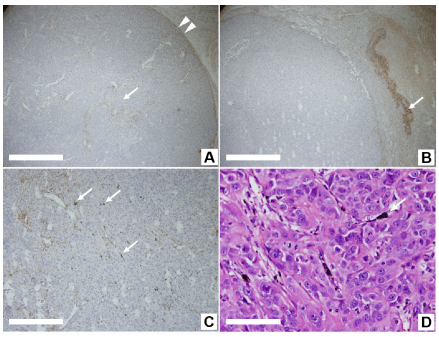

Fig. 3. Immunohistochemically stained images of macrophages in the xenograft tumor. (A) In the xenograft tumor not subjected to the injection of NS-loaded macrophages and laser irradiation, the stained innate macrophages are distributed along the tumor capsule (arrowheads) and around the vascular space within the tumor (arrow). The scale bar is 500 μm. (B) In the xenograft tumor injected with NS-loaded macrophages and exposed to PTT, the majority of injected macrophages stayed near the injection site, where the aggregated NSs are shown as black particles (arrow). The scale bar is 500 μm. (C) NSs aggregated into coarse particle of approximately 10 μm within the tumor mass after exposure to PTT (arrow). The scale bar is 200 μm. (D) Aggregated NSs are observed between cancer cells after exposure to PTT (arrow) and with H&E stain. The scale bar is 50 μm.

3.2 Photothermal treatment on xenograft tumors with NS-loaded macrophages

Before the administrating PTT, we performed control experiment of laser irradiation. The xenograft tumor mass was illuminated using a NIR laser at an irradiance of 1 W/cm^2 for 2 minutes without the injection of NS-loaded macrophages. Figure 4(A) is a photograph of a mouse with xenograft tumor (marked as a violet dot) where NS-loaded macrophages were not injected and Fig. 4(B) is the H&E stained image of a tissue section from the tumor site after the laser irradiation. The tumor was not affected by laser irradiation as the zoom-in image of the tumor area (inset in Fig. 4(B)) shows that the cellular structures were well preserved. On the other hand, the skin and subcutaneous tissues indicated as a blue box in Fig. 4(B) were detached from deep tissue around the tumor because of the edematous change resulting from the heat. We assessed the effect of PTT on both the intratumoral and the peritumoral injection groups. For the intratumoral injection group, NIR laser was illuminated on the tumor site at an irradiance of 1 W/cm^2 for 2 minutes. We observed that the tumor site with NS-loaded macrophages showed more swelling than the control site without them (Fig. 4(C)). Even if extensive and massive cellular destruction was observed within the tumor immediately after PTT, it occurred only in a partial portion of the tumor and mainly near the injection sites (Fig. 4(D)). Two weeks after PTT, the treated xenograft tumor had developed into hard and indurated tissues with a crust, and its growth appeared retarded compared with the xenograft tumor before PTT (Fig. 4(E)). In the tissue sections, although the majority of the remaining hard tissue consisted of fibrotic and dead cellular portions, live tumor cells were identified in other portions (Fig. 4(F)). This indicates that the PTT had failed to remove the entire tumor mass.

In the peritumoral injection group, the PTT caused the tumor with NS-loaded macrophages to swell in a similar way to the tissue swelling observed in the intratumoral group (Fig. 5(A)). In the tissue sections, extensive cellular destruction and separation was observed within the tumor immediately after PTT and the tumor was destroyed evenly and over all parts (Fig. 5(B)). Two weeks after PTT, the tumor site was nearly healed, leaving a certain amount of scarring and the tissue section showed only fibrotic tissue without tumor cells (Fig. 5(C), 5(D), and Visualization 1).

#254667 Received 27 Nov 2015; accepted 11 Dec 2015; published 18 Dec 2015

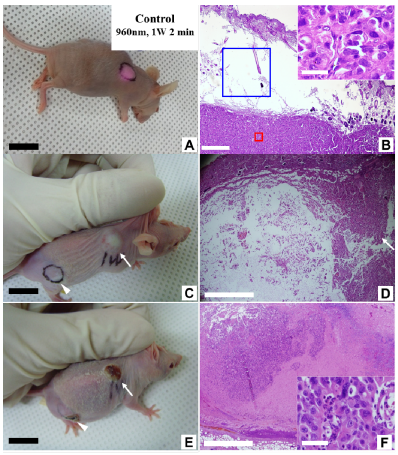

Fig. 4. The effect of PTT on the control and intratumoral injection groups. The xenograft tumor mass was illuminated using a NIR laser at an irradiance of 1 W/cm^2 for 2 minutes without (A and B) and with (C, D, E and F) the injection of NS-loaded macrophages. (A) A photograph of a mouse with xenograft tumor (marked as a violet dot) where NS-loaded macrophages were not injected. (B) The H&E stained image of a tissue section from the tumor site after the laser irradiation. The tumor was not affected by laser irradiation as the zoom-in image (inset in Fig. (B)) of the tumor area (marked as a red box) shows that the cellular structures were well preserved. On the other hand, the skin and subcutaneous tissues indicated as a blue box were detached from deep tissue around the tumor because of the edematous change resulting from the heat. (C) A photograph of a mouse with xenograft tumor (white arrow) to which NS-loaded macrophages were injected. (D) The H&E image of a tissue section from the tumor site immediately after administrating PTT. Extensive cellular destruction and dead spaces are evident on the left side of tumor interior, but the other portion shows intact tumor cells (white arrow). (E) A photograph of the same mouse in (C) taken after two weeks of the PTT. Larger and deeper crust formation occurred on the tumor site (white arrow). (F) The H&E stained image of a tissue section from the mouse in Fig. E. The degraded portion within the tumor displays acellular fibrotic tissue with dead cells. Live tumor cells were identified near the destructed portion. Scale bars in A, C and E corresponds to 1 mm, those in B, D and F are 500 μm, and the scale bars in their insets are 50 μm.

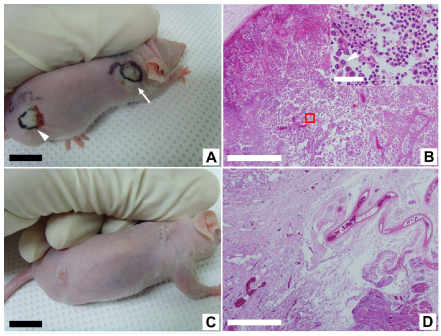

Fig. 5. The effect of PTT on the peritumoral injection group. The xenograft tumor mass was illuminated using a NIR laser at an irradiance of 1 W/cm^2 for 2 minutes after the injection of NS-loaded macrophages at four points surrounding the tumor. (A) Tumor with NS-loaded macrophages (arrow) shows swelling on the first day after PTT. Scale bar, 1 mm. (B) Extensive cellular destruction and dead spaces within the tumor immediately after undergoing PTT. The inset is zoom-up image as marked red box in (B). The H&E stain was used and the scale bars are 500 μm, and 50 μm. The majority of the tumor cells were destroyed and fragmented, and a portion of them showed the loss of intercellular connections (marked as an arrowhead). (C) Tumor site after PTT exhibit healed scars 2 weeks after PTT. Scale bar, 1 mm. (see Visualization 1) (D) Tumor site displaying fibrotic scar tissue 2 weeks after PTT. Scale bar, 500 μm.

#254667 Received 27 Nov 2015; accepted 11 Dec 2015; published 18 Dec 2015

4. Conclusion

We performed an *in vivo* study and confirmed the feasibility of PTT using macrophages as live cell vectors. We injected macrophages as nanoparticle carriers around the target region and showed that the NS-loaded macrophages effectively moved into xenograft tumors growing in live nude mice. Moreover, we verified that the photothermal effect of an NIR laser destroyed not only the macrophages themselves but also the neighboring cancer cells with minimal damage to the adjacent tissues.

From these studies, we could draw two additional conclusions that may need further attention and investigation. The first finding is that the efficiency of PTT depends on the way of injecting NS-loaded macrophages. We tested intratumoral and peritumoral injections, and found that the latter worked better than the former in that it removed the entire tumor mass. This difference could be explained by the histochemical analysis in which we found that the intratumoral injected macrophages remained concentrated near the injection sites while the peritumoral injected macrophages were relatively evenly spread out. Additional study clarifying the migration properties of macrophages is necessary to fully understand this discrepancy.

The second finding was about the cytotoxicity of the nanoparticles post treatment. After PTT, the NSs were aggregated into coarse particles with sizes of approximately 10μm that could not be passively distributed to other organs. This implies that the cytotoxicity induced by the diffusion of nanoparticles into healthy tissues and organs may not be a big issue for our local injection methods via macrophages.

With continuation of this study, we believe that PTT using NSs-loaded macrophages can become an alternative therapy for removing not only primary tumors, but also regional metastatic lymph nodes and distant metastatic sites since, unlike radiation therapy, this therapy can feasibility be performed repeatedly.

Acknowledgments

This research was supported by the Korea Health Technology R&D Project (HI14C0748) through the Korea Health Industry Development Institute (KHIDI) of the Ministry of Health & Welfare and a Grant-in-Aid for the Korea University Research and Business Foundation.